An RBF neural network–based MPPT with sliding mode and fuzzy control for PV systems using buck converter

Anh Van Le[1], Minh Van Pham[2], Linh Thi To Vu[3]
[1]Department of Industrial and Civil Electrical Engineering, Faculty of Electrical-Automation, University of Economics-Technology for Industries, Hanoi, Vietnam
[2]Department of Electrical Engineering, Faculty of Electrical-Automation, University of Economics-Technology for Industries, Hanoi, Vietnam
[3]Administrative Affairs Office, University of Economics-Technology for Industries, Hanoi, Vietnam

Article Info

Article history:

Received Nov 5, 2025
Revised Mar 20, 2026
Accepted Apr 19, 2026

Keywords:

Buck converter
Fuzzy logic
Photovoltaic system
Radial basis function
Sliding mode control

ABSTRACT

This paper proposes an integrated control strategy for maximum power point tracking (MPPT) in photovoltaic (PV) systems using a buck converter. The controller combines a radial basis function (RBF) neural network for uncertainty approximation, sliding mode control (SMC) for robustness, and fuzzy logic for adaptive tuning of the switching gain to reduce chattering. The complete RBF–SMC–fuzzy control law is derived, and closed-loop stability is proven using Lyapunov theory. Simulation results in MATLAB/Simulink under both resistive and battery charging loads show that the proposed method achieves fast tracking with a settling time of about 20 ms, a tracking efficiency higher than 99%, and a voltage ripple of approximately 1.2%. Compared with conventional methods, the proposed controller significantly reduces chattering and improves power extraction performance under irradiance and load variations.

Corresponding Author:

Minh Van Pham
Department of Electrical Engineering, Faculty of Electrical-Automation
University of Economics-Technology for Industries
Hanoi, Vietnam
Email: pvminh@uneti.edu.vn

1. INTRODUCTION

The increasing demand for renewable energy has intensified the need for efficient photovoltaic (PV) power conversion systems [1], [2]. However, due to the nonlinear characteristics of PV modules, the maximum power point (MPP) varies with irradiance and temperature, which makes reliable maximum power point tracking (MPPT) a critical challenge [3]–[5].

Conventional MPPT methods such as perturb and observe (P&O) and incremental conductance (IncCond) are widely used because of their simplicity and low computational cost, but they often suffer from slow convergence, steady-state oscillations, and poor performance under rapidly changing irradiance or partial shading conditions [6], [7]. To address these limitations, advanced MPPT techniques based on fuzzy logic, neural networks, and sliding mode control (SMC) have been widely investigated [8]–[12]. Fuzzy controllers improve adaptability but require extensive tuning and lack stability guarantees. RBF neural networks can approximate nonlinear PV dynamics but may suffer from limited robustness, while SMC provides strong robustness against uncertainties at the expense of chattering effects [8], [13]–[17].

Recent studies have further explored intelligent control strategies to enhance PV system performance. For instance, nonlinear autoregressive with eXogenous inputs (NARX)-radial basis function (RBF) neural networks have been applied to hybrid energy storage systems in microgrids, enabling improved prediction capability and adaptive energy management under fluctuating renewable generation conditions [18]. Comparative studies on RBF neural network-based MPPT algorithms have also been conducted for different direct current (DC)–DC converter topologies, demonstrating improved tracking accuracy and dynamic response compared with conventional MPPT approaches [19]. Furthermore, fuzzy logic-based MPPT controllers implemented in three-level DC–DC converters have shown improved steady-state performance and reduced oscillations in PV applications [20]. Advanced type-2 fuzzy logic control strategies have also been proposed for multi-level quadratic boost converters, providing enhanced robustness against parameter uncertainties and environmental disturbances [21]. In addition, neural-network-based optimization techniques have been employed to improve the efficiency of multi-level boost converters in PV systems, achieving higher energy conversion efficiency and improved dynamic performance [22]. Although hybrid control schemes combining SMC with fuzzy logic or neural networks have been proposed to alleviate chattering and improve adaptation [11], [12], [23], [24], several open issues remain. Most existing designs neglect parameter variations in the converter or PV module, assume ideal sensor conditions, or rely on fixed control gains that limit performance under rapidly changing irradiance. Moreover, fuzzy tuning alone may be insufficient to compensate for unmodeled nonlinearities, while RBF-based schemes without switching adaptation may exhibit slow response and degraded transient accuracy.

Furthermore, many existing hybrid MPPT strategies address nonlinear approximation and controller gain tuning separately. In fuzzy–SMC approaches, fuzzy logic is typically used to regulate switching gains without explicitly compensating for unknown nonlinear dynamics of the PV–converter system. Conversely, RBF-based MPPT methods mainly focus on approximating nonlinear system behavior while relying on fixed control parameters, which may limit robustness under rapidly changing environmental conditions. Therefore, an integrated adaptive control framework capable of simultaneously addressing nonlinear uncertainties, gain adaptation, and robustness enhancement remains an important research challenge. Despite these advances, recent findings indicate that under harsh operating conditions—such as rapidly changing irradiance, partial shading, and measurement noise—traditional MPPT methods, as well as standalone artificial intelligence (AI)-based techniques, may still fail to deliver satisfactory efficiency [14], [24], [25]. This motivates the integration of adaptive RBF networks with SMC, which can simultaneously guarantee robustness and enhance tracking accuracy [15]–[17]. Unlike prior hybrid MPPT controllers, the approach proposed in this paper integrates adaptive RBF approximation with a SMC structure whose switching gain is dynamically tuned through a fuzzy logic mechanism. In this coordinated framework, the RBF neural network estimates the unknown nonlinear dynamics of the PV–converter system in real time, while the sliding mode controller guarantees robust convergence in the presence of parameter uncertainties and disturbances. Meanwhile, the fuzzy logic mechanism dynamically regulates the switching gain to suppress chattering without sacrificing robustness. Furthermore, the stability of the overall closed-loop system is rigorously analyzed using Lyapunov theory, ensuring boundedness of all signals and convergence toward the maximum power operating point. Such a robust MPPT strategy is particularly important for practical renewable energy applications, including standalone PV systems, PV–battery charging systems, and microgrid-based distributed energy systems where environmental conditions and load demand frequently change. By improving tracking accuracy and reducing steady-state power oscillations, the proposed control approach can enhance energy harvesting efficiency and improve the reliability of power electronic converters used in modern PV energy systems.

Building on this motivation, this paper proposes an integrated RBF–SMC–fuzzy control strategy for PV MPPT systems. In the proposed method, the RBF network adaptively estimates the nonlinear and uncertain dynamics of the PV–converter system, the SMC structure guarantees robust convergence under parameter perturbations, and the fuzzy logic mechanism dynamically regulates the switching gain to suppress chattering. The main objectives are to: i) accelerate convergence toward the MPP, ii) minimize steady-state power oscillations, and iii) maintain robustness against parameter uncertainties, measurement noise, and rapid irradiance fluctuations.

2. METHOD

2.1. Mathematical model of the photovoltaic–buck converter

Accurate mathematical modeling is essential for developing effective control strategies in PV systems. In the configuration considered, a PV array supplies energy to a buck converter, which regulates the operating point of the PV source to extract maximum power. This subsection presents the nonlinear electrical model of the PV module, the averaged dynamic model of the buck converter, and the unified system representation suitable for control design.

The PV module is commonly represented by the single-diode equivalent circuit, which provides an appropriate balance between model accuracy and computational simplicity. The output current of the PV array can be expressed as (1):

$$I_{pv} = I_{ph} - I_0 \left(e^{\frac{q(V_{pv}+I_{pv}R_s)}{nkT}} - 1 \right) - \frac{V_{pv} + I_{pv}R_s}{R_{sh}}, \tag{1}$$

where V_{pv} and I_{pv} denote the PV terminal voltage and current, respectively. The parameters include the photocurrent I_{ph}, reverse saturation current I_0, series resistance R_s, shunt resistance R_{sh}, diode ideality factor n, temperature T, electron charge q, and Boltzmann constant k. In (1) captures the nonlinear I–V characteristic of the PV module and the existence of a unique MPP.

To interface the PV array with the load, a buck converter is employed owing to its simple structure and high efficiency. Let i_L be the inductor current, v_o the output voltage, and $d \in [0, 1]$ the duty ratio of the pulse–width modulation signal. The schematic structure of the PV–buck converter considered in this study is illustrated in Figure 1. The converter regulates the PV operating voltage through the duty ratio of the switching device.

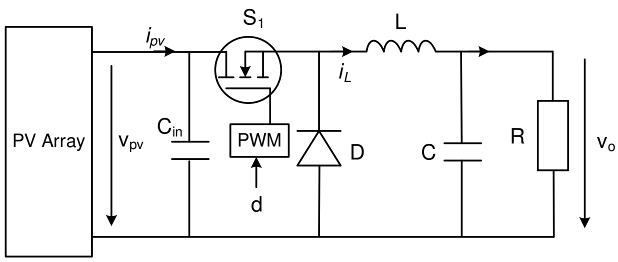

Figure 1. Schematic diagram of the PV–buck converter system used in the proposed MPPT framework

By applying Kirchhoff's laws and using the averaged modeling approach, the dynamics of the buck converter are given by (2):

$$L\frac{di_L}{dt} = V_{pv} - (1-d)v_o, \qquad C\frac{dv_o}{dt} = (1-d)i_L - \frac{v_o}{R}, \tag{2}$$

where L, C, and R represent the inductance, output capacitance, and load resistance, respectively. By combining the PV source model with the converter equations, the overall system can be expressed in a compact nonlinear form:

$$\dot{x} = f(x) + g(x)u + \delta(t), \tag{3}$$

with the state and control input defined as $x = [i_L, v_o]^T, \quad u = d$. Here, $f(x)$ and $g(x)$ denote the intrinsic nonlinear dynamics of the converter, while $\delta(t)$ captures parameter uncertainties and external disturbances.

2.2. Control problem formulation

The control objective of the MPPT problem is to regulate the duty ratio $d(t)$ such that the instantaneous PV output power $P_{pv}(t) = V_{pv}(t)I_{pv}(t)$ tracks the MPP value $P_{mpp}(t)$ corresponding to the optimal voltage reference $V_{ref}(t)$. In other words, the controller continuously adjusts $d(t)$ to drive the PV operating point toward $V_{ref}(t)$, where P_{pv} reaches its peak value under varying irradiance and temperature conditions. Because the PV–buck system exhibits strong nonlinearity and is subject to parameter uncertainties and environmental disturbances, conventional linear controllers fail to maintain accurate power tracking. Hence, an adaptive and robust control strategy is required to guarantee reliable MPP regulation under time-varying and uncertain conditions. This motivates the development of the integrated RBF–SMC–fuzzy controller described in the following section.

2.3. Integrated RBF–SMC–fuzzy controller design

Designing an MPPT controller that is both robust and smooth requires combining three complementary features: i) adaptive approximation of unknown dynamics, ii) robust sliding-mode convergence, and iii) chattering reduction via fuzzy gain scheduling. This subsection presents the control architecture, RBF approximation mechanism, fuzzy gain regulation, and the resulting control law.

2.3.1. Control objective and sliding surface

The control objective is to regulate the PV terminal voltage V_{pv} so that it tracks a reference $V_{ref}(t)$ corresponding to the MPP. Define the tracking error $e(t) = V_{pv}(t) - V_{ref}(t)$. A first-order sliding surface is selected as (4):

$$s(t) = \dot{e}(t) + \lambda e(t), \qquad \lambda > 0, \tag{4}$$

where λ determines the desired convergence rate of the voltage tracking error. When $s(t) \to 0$, both $e(t)$ and $\dot{e}(t)$ tend to zero, implying exponential convergence of V_{pv} to V_{ref}. The linear sliding surface in (4) is chosen because it offers a good balance between simplicity, fast convergence, and ease of stability analysis. Unlike higher-order or nonlinear sliding manifolds that require additional state derivatives, the first-order form ensures a straightforward Lyapunov proof and is well suited for real-time MPPT control where only V_{pv} and I_{pv} are measurable. Moreover, the parameter λ allows flexible adjustment of the dynamic response: larger λ yields faster error convergence, while smaller λ provides smoother control with reduced switching effort.

2.3.2. Radial basis function neural network for uncertainty approximation

Assume the system dynamics can be written in the form (as in (3))

$$\dot{x} = f(x) + g(x)u + \Delta(x,t), \tag{5}$$

where $\Delta(x,t)$ represents unknown nonlinearities and disturbances.

Adopt a RBF neural network to approximate the unknown nonlinear term $\Delta(x,t)$. The RBF neural network employed in this work adopts a three-layer feedforward structure consisting of an input layer, a hidden layer with radial basis neurons, and a linear output layer. The input layer receives the system state vector $x = [i_L, v_o]^T$. In the hidden layer, each neuron computes a Gaussian RBF.

$$\varphi_j(x) = \exp\left(-\frac{\|x - c_j\|^2}{2\sigma_j^2}\right), \tag{6}$$

where c_j and σ_j denote the center and width of the jth basis function. The output layer performs a linear combination of hidden-layer outputs to produce the approximation.

$$\hat{\Delta}(x,t) = \sum_{j=1}^{m} \hat{W}_j \varphi_j(x), \tag{7}$$

which can be written compactly as (8):

$$\hat{\Delta}(x,t) = \hat{W}^\top \varphi(x), \tag{8}$$

where $\varphi(x) = [\varphi_1(x), \ldots, \varphi_m(x)]^\top$ and $\hat{W} \in \mathbb{R}^m$ are adaptive weights.

The weight adaptation is governed by a gradient-like learning law augmented with projection to maintain bounded estimates:

$$\dot{\hat{W}} = \gamma\, \varphi(x)\, s - \Pi(\hat{W}), \tag{9}$$

where $\gamma > 0$ is the learning gain and $\Pi(\cdot)$ denotes a projection operator that enforces $\|\hat{W}\| \leq W_{\max}$. The projection is implemented so that when $\|\hat{W}\| > W_{\max}$ the update is modified to prevent further growth. Assume there exists an ideal weight vector W^* and a bounded residual such that:

$$\Delta(x,t) = W^{*\top} \varphi(x) + \varepsilon(x,t), \qquad \|\varepsilon(x,t)\| \leq \varepsilon_{\max}. \tag{10}$$

2.3.3. Fuzzy gain scheduler

To mitigate chattering while retaining robustness, adopt a fuzzy inference system (FIS) that adjusts the switching gain K_f in real time based on the sliding variable and its rate: $K_f = \mathrm{FIS}\big(\|s\|, \|\dot{s}\|\big)$.

Inputs are $X_1 = \|s\|$ and $X_2 = \|\dot{s}\|$. Use three triangular membership functions for each input: Small (S), Medium (M), Large (L). The output is ΔK (increment to a baseline K_0), and $K_f = K_0 + \Delta K$ is clamped to $K_{\min} \leq K_f \leq K_{\max}$. A compact 3-by-3 fuzzy rule base is given in Table 1.

Table 1. Fuzzy rule base for adaptive switching gain K_f

$\|s\|\backslash\|\dot{s}\|$	S	M	L
S	$\Delta K = -k_s$	$\Delta K = 0$	$\Delta K = k_m$
M	$\Delta K = 0$	$\Delta K = k_m$	$\Delta K = k_b$
L	$\Delta K = k_m$	$\Delta K = k_b$	$\Delta K = k_b$

where $k_s < 0$, $k_m > 0$, and $k_b > k_m$ are design constants. Mamdani inference with centroid defuzzification is recommended.

2.4. Control law

By differentiating $s(t)$ and substituting (3), the sliding dynamics can be expressed as (11):

$$\dot{s} = b(x)u + q(x,t), \tag{11}$$

where $b(x) > 0$ is the equivalent control gain and $q(x,t)$ collects all remaining terms including $\Delta(x,t)$. The control input $u = d(t)$ (i.e., the duty ratio) is then defined as (12):

$$u = -\frac{1}{b(x)}\Big(\hat{\Delta}(x,t) + K_f(s,\dot{s})\,\mathrm{sat}\Big(\frac{s}{\phi}\Big)\Big), \tag{12}$$

where $\phi > 0$ defines the boundary layer thickness and $\mathrm{sat}(z)$ is a continuous approximation of the sign function:

$$\mathrm{sat}(z) = \begin{cases} \mathrm{sgn}(z), & \|z\| > 1, \\ z, & \|z\| \leq 1. \end{cases} \tag{13}$$

Substituting (12) into (11) yields the closed-loop sliding dynamics

$$\dot{s} = -K_f(s,\dot{s})\,\mathrm{sat}\Big(\frac{s}{\phi}\Big) + \tilde{\Delta}(x,t), \tag{14}$$

where $\tilde{\Delta}(x,t) = \Delta(x,t) - \hat{\Delta}(x,t)$ denotes the residual approximation error.

Remark 1 *For implementation, $\dot{s}$ should be filtered to reduce sensor noise before entering the fuzzy module. The boundary layer ϕ must be selected small enough for accurate tracking yet large enough to avoid chattering due to quantization or sampling. Moreover, the parameters $W_{\max}$ and γ must balance adaptation speed and stability, with projection ensuring bounded neural weights.*

Remark 2 *The RBF neural network employs a compact structure with a limited number of radial basis neurons to approximate the nonlinear PV–converter dynamics. The fuzzy inference system uses a small rule base to regulate the switching gain of the sliding mode controller based on the sliding surface and its derivative. This configuration enables effective uncertainty compensation and chattering suppression while maintaining low computational complexity suitable for real-time implementation.*

The implementation procedure of the proposed RBF–SMC–fuzzy MPPT controller is summarized in Algorithm 1, which outlines the sequential operations performed at each sampling instant.

Algorithm 1. RBF–SMC–fuzzy MPPT control algorithm

```
Initialize parameters λ, φ, γ, W_max, K_0
loop
    Measure PV voltage V_pv and current I_pv
    Compute reference voltage V_ref
    Compute tracking error
```

$$e = V_{pv} - V_{ref}$$

```
    Compute sliding surface
```

$$s = \dot{e} + \lambda e$$

```
    Estimate uncertainty using RBF network
```

$$\hat{\Delta}(x,t) = \hat{W}^\top \varphi(x)$$

```
    Update neural weights
```

$$\dot{\hat{W}} = \gamma \varphi(x) s - \Pi(\hat{W})$$

```
    Compute adaptive switching gain
```

$$K_f = \mathrm{FIS}(\|s\|, \|\dot{s}\|)$$

```
    Compute duty ratio
```

$$d = -\frac{1}{b(x)} \left(\hat{\Delta}(x,t) + K_f \,\mathrm{sat}\left(\frac{s}{\phi}\right)\right)$$

```
    Update PWM duty cycle
end loop
```

2.5. Stability analysis

Stability is established using Lyapunov analysis. Consider the candidate function:

$$V(s, \tilde{W}) = \frac{1}{2}s^2 + \frac{1}{2\gamma}\tilde{W}^\top \tilde{W}, \tag{15}$$

where $\tilde{W} = W^* - \hat{W}$ is the weight estimation error. Differentiating (15) along the trajectories of (14) and using (9) gives

$$\dot{V} = s\dot{s} - \frac{1}{\gamma}\tilde{W}^\top \dot{\hat{W}} = s\Big(- K_f \,\mathrm{sat}\big(\tfrac{s}{\phi}\big) + \tilde{\Delta}\Big) - \tilde{W}^\top \varphi\, s + \frac{1}{\gamma}\tilde{W}^\top \Pi(\hat{W}). \tag{16}$$

Using (10), we have $\tilde{\Delta} = \varepsilon + \tilde{W}^\top \varphi$, which simplifies (16) to

$$\dot{V} = -sK_f \,\mathrm{sat}(s/\phi) + s\varepsilon + \frac{1}{\gamma}\tilde{W}^\top \Pi(\hat{W}). \tag{17}$$

Since $\tilde{W}^\top \Pi(\hat{W}) \leq 0$ by design of the projection, it follows that

$$\dot{V} \leq -sK_f \,\mathrm{sat}(s/\phi) + \|s\|\, \varepsilon_{\max}. \tag{18}$$

Using the inequality $s\,\mathrm{sat}(s/\phi) \geq \|s\| - \phi$, we obtain

$$\dot{V} \leq -(K_f - \varepsilon_{\max})\|s\| + K_f \phi. \tag{19}$$

If $K_f(t) > \varepsilon_{\max}$, $\dot{V} < 0$ whenever $\|s\| > \frac{K_f \phi}{K_f - \varepsilon_{\max}}$, implying that $s(t)$ enters the compact set

$$\mathcal{S} = \left\{ s : \|s\| \leq \frac{K_f \phi}{K_f - \varepsilon_{\max}} \right\}.$$

Since K_f is bounded, all closed-loop signals are uniformly ultimately bounded, and $s(t)$ converges to a small neighborhood of zero. By using sufficiently rich RBF bases (small $\varepsilon_{\max}$) and a thin boundary layer ϕ, this neighborhood can be made arbitrarily small. In the ideal case $\varepsilon_{\max} \to 0$ and $\phi \to 0$, asymptotic convergence $s(t) \to 0$ is achieved.

3. RESULTS AND DISCUSSION

The performance of the proposed RBF–SMC–fuzzy MPPT control scheme was evaluated through detailed simulations in MATLAB/Simulink. A 2000 W PV array, modeled using the single-diode equivalent circuit, was connected to a buck converter operating at a switching frequency of 10 kHz. The converter parameters were set as $L = 7$ mH, $C = 108$ μF, $C_{in} = 470$ μF, and $R = 1.2$ Ω. To examine robustness, the inductance L and load resistance R were varied by $\pm 20\%$ from their nominal values during the simulations. The PV array consisted of two parallel strings, each composed of four series-connected panels with open-circuit voltage $V_{oc} = 36.3$ V, short-circuit current $I_{sc} = 7.84$ A, and MPP values of $V_{mp} = 29$ V and $I_{mp} = 7.35$ A. The irradiance profile used in the simulations consists of step changes from 1000 $\mathrm{W/m^2}$ to 500 $\mathrm{W/m^2}$ at $t = 0.5$ s. Gaussian measurement noise with a standard deviation of 0.5% was also introduced to emulate sensor uncertainty. A fixed-step discrete solver with a sampling interval of $\Delta t = 100$ μs was used to emulate the real-time behavior of a digital controller. The complete simulation model was developed using Simscape Electrical, as illustrated in Figure 2, to ensure realistic representation of converter switching and PV characteristics.

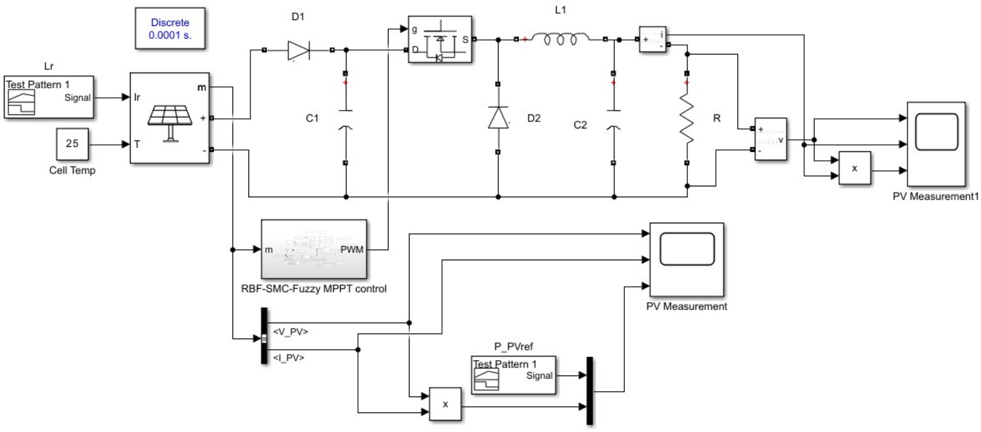

Figure 2. Simulink–Simscape model of the proposed RBF–SMC–fuzzy control system

The RBF neural network employed five Gaussian basis nodes distributed uniformly across the PV voltage range of 10–100 V, each with width $\sigma_j = 3$. The adaptive learning rate was set to $\gamma = 10$, and the neural weights were limited by a projection bound of $W_{\max} = 10$ to ensure numerical stability. In the SMC design, $\lambda = 20$ was selected for the sliding surface slope and $\phi = 0.05$ for the boundary layer thickness. A fuzzy inference mechanism dynamically tuned the switching gain K_f according to $|s|$ and $|\dot{s}|$ using three triangular membership functions—*Small*, *Medium*, and *Large*. This structure allowed the controller to balance fast convergence with reduced chattering during steady-state operation.

Two load scenarios were simulated to validate control performance: i) a purely resistive load and ii) a nonlinear battery charging load. Unless otherwise specified, simulations were conducted under standard test conditions to analyze transient speed, steady-state precision, and robustness to irradiance variations.

3.1. Scenario 1: resistive load

Figures 3(a)–(c) show the PV voltage, current, and power under a resistive load during irradiance variation. The proposed RBF–SMC–fuzzy controller accurately regulates the PV voltage to its MPP reference and achieves convergence within approximately 40 ms after each change. Both current and power exhibit smooth transitions with minimal overshoot and low steady-state ripple, indicating stable MPPT operation under varying environmental conditions.

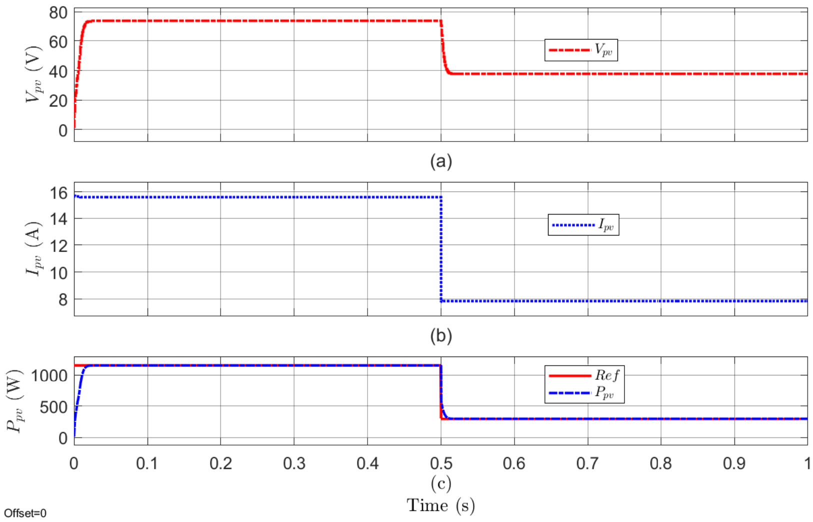

Figure 3. PV voltage, current, and power under resistive load with irradiance variation: (a) PV voltage, (b) PV current, and (c) PV power

3.2. Scenario 2: battery charging load

In this case, the PV–buck converter charges a 48 V/100 A battery characterized by nonlinear voltage–current behavior. Figure 4 shows the PV power tracking, while Figures 5(a) and (b) present the battery voltage and current profiles. The controller maintains PV operation close to the MPP across both irradiance levels with negligible steady-state deviation. The PV power tracks the reference within approximately 20 ms after each irradiance change, while the battery voltage and current remain stable and smooth, indicating reliable energy transfer during the charging process.

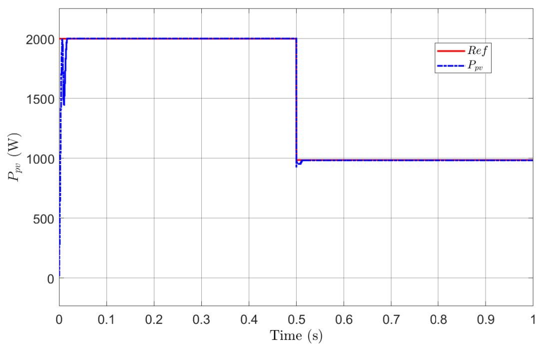

Figure 4. PV power response under battery charging conditions during irradiance change

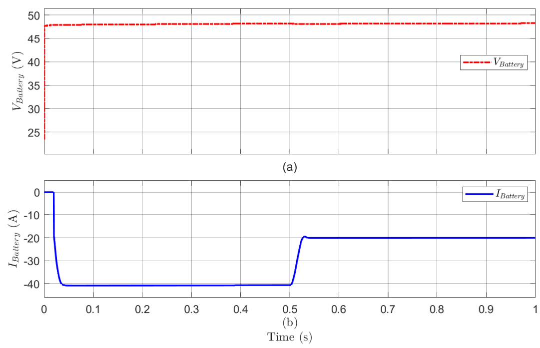

Figure 5. Battery charging characteristics during irradiance change: (a) battery voltage and (b) battery current

3.3. Comparative evaluation

To benchmark performance, the proposed controller was compared with two widely used MPPT strategies: the conventional P&O and the classical SMC-based algorithms. All controllers were implemented under identical converter parameters and PV conditions to ensure a fair comparison. The key performance metrics—including settling time, voltage ripple, tracking efficiency, and chattering amplitude—are summarized in Table 2.

Table 2. Quantitative comparison of MPPT performance under resistive load

Metric	P&O	Classical SMC	Proposed RBF–SMC–fuzzy
Settling time (ms)	120	58	20
Voltage ripple (%)	4.1	2.3	1.2
Tracking efficiency (%)	93.8	96.8	99.2
Chattering amplitude (V)	0.85	0.46	0.16

The second and third rows of Table 2 represent the measured voltage ripple and tracking efficiency, respectively. For quantitative comparison, the relative improvement for a performance metric M is calculated as $\mathrm{Improvement}(\%) = \frac{M_{\text{baseline}} - M_{\text{proposed}}}{M_{\text{baseline}}} \times 100$, where M_{baseline} and M_{proposed} denote the metric values of the baseline (P&O or SMC) and proposed controllers. Similarly, the chattering reduction rate is defined as $\mathrm{Reduction}_{\text{chat}}(\%) = \frac{A_{\text{baseline}} - A_{\text{proposed}}}{A_{\text{baseline}}} \times 100$. According to Table 2, the proposed method reduces chattering by approximately 81.2% compared with P&O and 65.2% compared with classical SMC.

As summarized in Table 2, the proposed RBF–SMC–fuzzy controller outperforms both P&O and classical SMC across all performance metrics, achieving the shortest settling time, the lowest voltage ripple, and the highest tracking efficiency. When the irradiance decreases from $1000\ \mathrm{W/m^2}$ to $500\ \mathrm{W/m^2}$, the controller reacquires the new MPP within 20 ms, whereas P&O and SMC exhibit noticeable oscillations before reaching steady state. These results demonstrate the superior dynamic performance, robustness, and steady-state accuracy of the proposed MPPT strategy under varying operating conditions. To assess statistical robustness, the simulations were repeated under multiple irradiance transition scenarios with random variations. The average MPPT efficiency remained above 99% with a standard deviation below 0.3%, indicating consistent controller performance. To evaluate the robustness of the proposed controller, a sensitivity analysis was conducted by varying key controller parameters, including the RBF neural network learning rate γ and the fuzzy gain parameters. Additional simulations were performed by perturbing these parameters within $\pm 20\%$ of their nominal values. The results indicate that the proposed RBF–SMC–fuzzy controller maintains stable MPPT operation with small steady-state oscillations under these parameter variations, while preserving a tracking efficiency above $\pm 98.5\%$. This confirms the robustness of the proposed control strategy against controller parameter uncertainties.

To further illustrate the contribution of each component, an ablation study was conducted by progressively integrating the RBF neural network and fuzzy gain tuning into the baseline SMC controller. As shown in Table 3, the RBF neural network enhances the compensation of nonlinear PV–converter dynamics, improving tracking efficiency, while the fuzzy gain tuning mechanism mitigates voltage oscillations caused by switching chattering. By combining these complementary mechanisms with the inherent robustness of SMC, the proposed RBF–SMC–fuzzy controller achieves improved tracking performance and reduced steady-state ripple.

Table 3. Component contribution analysis of the proposed RBF–SMC–fuzzy MPPT controller

Controller configuration	Efficiency (%)	Voltage ripple (%)
SMC only	95.8	2.6
SMC+RBF	98.1	2.1
SMC+fuzzy	96.9	1.6
Proposed RBF–SMC–fuzzy	99.2	1.2

3.4. Discussion

The simulation outcomes demonstrate that the proposed RBF–SMC–fuzzy MPPT controller achieves a desirable balance between robustness, adaptability, and smoothness. The improved tracking performance arises from the complementary roles of the three control layers: SMC ensures robust convergence, the RBF network compensates system uncertainties, and the fuzzy mechanism suppresses switching chattering. By combining the sliding-mode robustness, neural adaptive estimation, and fuzzy gain regulation, the controller exhibits excellent disturbance rejection while significantly mitigating chattering—a common issue in high-frequency switching control. The RBF neural network enhances uncertainty compensation by approximating unknown nonlinear dynamics in the PV–converter system. Through adaptive estimation of these uncertainties, the controller reduces modeling errors and improves voltage regulation accuracy near the MPP. Both resistive and nonlinear battery load tests validate that the proposed approach can sustain high tracking accuracy and stable operation under realistic irradiance variations. Although the proposed controller shows robust MPPT performance under the tested irradiance variations, extreme conditions such as severe partial shading or rapid temperature fluctuations may introduce additional nonlinearities and dynamic disturbances. In such scenarios, the controller may require further adaptation mechanisms or enhanced estimation strategies to maintain optimal tracking performance.

Remark 3 *The computational complexity of the proposed RBF–SMC–fuzzy controller mainly involves the evaluation of Gaussian RBFs and fuzzy inference for switching gain regulation. These operations require only basic arithmetic computations and can be efficiently implemented on modern digital control platforms such as DSP or FPGA-based systems, making the proposed method suitable for real-time PV power conversion applications.*

4. CONCLUSION

An integrated RBF–SMC–fuzzy control strategy for PV MPPT is proposed, combining sliding-mode robustness, RBF-based nonlinear approximation, and fuzzy gain tuning to achieve fast tracking with reduced chattering. Simulation results under both resistive and battery charging loads demonstrate high tracking efficiency (above 99%) with reduced voltage ripple and improved transient performance. More specifically, the proposed controller achieves a settling time of approximately 20 ms following irradiance transitions, a voltage ripple of about 1.2%, and a significant reduction of chattering amplitude compared with conventional MPPT approaches. Overall, the proposed RBF–SMC–fuzzy controller provides a robust and computationally efficient MPPT solution suitable for real-time PV energy conversion systems. Although the proposed controller shows promising simulation results, several practical aspects should be considered for real-world implementation. Sensor noise in voltage and current measurements may affect MPPT accuracy, and switching stress in power electronic devices requires further evaluation. Future work will therefore focus on experimental validation using real PV hardware, including tests under sensor noise and partial shading conditions, as well as assessment of switching stress and overall system efficiency.

ACKNOWLEDGMENTS

The authors gratefully acknowledge the Faculty of Electrical–Automation, University of Economics–Technology for Industries (UNETI), Hanoi, Vietnam, for providing a supportive research environment for this work.

FUNDING INFORMATION

Authors state no funding involved.

AUTHOR CONTRIBUTIONS STATEMENT

This journal uses the Contributor Roles Taxonomy (CRediT) to recognize individual author contributions, reduce authorship disputes, and facilitate collaboration.

Name of Author	C	M	So	Va	Fo	I	R	D	O	E	Vi	Su	P	Fu
Anh Van Le	✓	✓	✓	✓	✓	✓	✓	✓	✓	✓			✓	
Minh Van Pham	✓	✓	✓		✓	✓		✓	✓	✓	✓	✓		
Linh Thi To Vu	✓		✓	✓		✓			✓	✓	✓		✓	✓

C : **C**onceptualization
M : **M**ethodology
So : **So**ftware
Va : **Va**lidation
Fo : **Fo**rmal Analysis
I : **I**nvestigation
R : **R**esources
D : **D**ata Curation
O : Writing - **O**riginal Draft
E : Writing - Review & **E**diting
Vi : **Vi**sualization
Su : **Su**pervision
P : **P**roject Administration
Fu : **Fu**nding Acquisition

CONFLICT OF INTEREST STATEMENT

Authors state no conflict of interest.

DATA AVAILABILITY

Data availability is not applicable to this paper as no new data were created or analyzed in this study.

REFERENCES

[1] D. Shetty, N. S. Jayalakshmi, M. Arjun, and P. Hebbar, "Evaluation of MPPT algorithms for PV system under partial shading conditions," in *2022 International Conference on Intelligent Controller and Computing for Smart Power (ICICCSP)*, Hyderabad, India, 2022, pp. 1–6, doi: 10.1109/ICICCSP53532.2022.9862362.

[2] W. Xiao, A. Elnosh, V. Khadkikar, and H. Zeineldin, "Overview of maximum power point tracking technologies for photovoltaic power," in *IECON 2011-37th Annual Conference of the IEEE Industrial Electronics Society*, Melbourne, VIC, Australia, 2011, pp. 3900–3905, doi: 10.1109/IECON.2011.6119946.

[3] A. Safari and S. Mekhilef, "Implementation of incremental conductance method with direct control," in *TENCON 2011-2011 IEEE Region 10 Conference*, Bali, Indonesia, 2011, pp. 944–948, doi: 10.1109/TENCON.2011.6129249.

[4] N. Kumar, I. Hussain, B. Singh, and B. K. Panigrahi, "Single sensor-based MPPT of partially shaded PV system for battery charging by using cauchy and gaussian sine cosine optimization," *IEEE Transactions on Energy Conversion*, vol. 32, no. 3, pp. 983–992, 2017, doi: 10.1109/TEC.2017.2669518.

[5] M. A. Eltawil and Z. Zhao, "MPPT techniques for photovoltaic applications," *Renewable and Sustainable Energy Reviews*, vol. 25, pp. 793–813, 2013, doi: 10.1016/j.rser.2013.05.022.

[6] F. Belhachat and C. Larbes, "A review of global maximum power point tracking techniques of photovoltaic system under partial shading conditions," *Renewable and Sustainable Energy Reviews*, vol. 92, pp. 513–553, 2018, doi: 10.1016/j.rser.2018.04.094.

[7] Y.-H. Liu, C.-L. Liu, J.-W. Huang, and J.-H. Chen, "Neural-network-based maximum power point tracking methods for photovoltaic systems operating under fast changing environments," *Solar Energy*, vol. 89, pp. 42–53, 2013, doi: 10.1016/j.solener.2012.11.017.

[8] Z. A. Khan, L. Khan, S. Ahmad, S. Mumtaz, M. Jafar, and Q. Khan, "RBF neural network based backstepping terminal sliding mode MPPT control technique for PV system," *PLoS ONE*, vol. 16, no. 4, 2021, doi: 10.1371/journal.pone.0249705.

[9] H. Khaterchi, L. Gafssaoui, J. Chrouta, and A. Zaafouri, "Sliding mode control of photovoltaic systems," in *2022 IEEE International Conference on Electrical Sciences and Technologies in Maghreb (CISTEM)*, Tunis, Tunisia, 2022, vol. 4, pp. 1–6, doi: 10.1109/CISTEM55808.2022.10043974.

[10] H. G. Ali and R. V. Arbos, "Chattering free adaptive sliding mode controller for photovoltaic panels with maximum power point tracking," *Energies*, vol. 13, no. 21, 2020, doi: 10.3390/en13215678.

[11] S. Marhraoui, A. Abbou, N. El Hichami, S. E. Rhaili, and S. Krit, "Fuzzy sliding mode hybrid control MPPT strategy and PI control as a controller for a battery integrated with PV system," *Journal of Advanced Research in Dynamical and Control Systems*, vol. 12, no. 1, pp. 415–428, 2020, doi: 10.5373/JARDCS/V12SP1/20201089.

[12] M. Aly and H. Rezk, "An improved fuzzy logic control-based MPPT method to enhance the performance of PEM fuel cell system," *Neural Computing and Applications*, vol. 34, no. 6, pp. 4555–4566, 2022, doi: 10.1007/s00521-021-06611-5.

[13] F. A. Banakhr and M. I. Mosaad, "High performance adaptive maximum power point tracking technique for off-grid photovoltaic systems," *Scientific Reports*, vol. 11, no. 1, 2021, doi: 10.1038/s41598-021-99949-8.

[14] Z. Li, G. Dewantoro, T. Xiao, and A. Swain, "A comparative analysis of fuzzy logic control and model predictive control in photovoltaic maximum power point tracking," *Electronics*, vol. 14, no. 5, pp. 1-18, 2025, doi: 10.3390/electronics14051009.

[15] L. Zaghba, A. Borni, M. K. Benbitour, and A. Fezzani, "A Hybrid RBFNN-PI MPPT Controller for Optimal Energy Harvesting in PV Systems under Changing Environmental Conditions," *Journal of Renewable Energies*, vol. 28, no. 2, pp. 277–301, 2025, doi: 10.54966/jreen.v28i2.1441.

[16] A. Guerbouz, I. Merzouk, W. M. Kacemi, A. M. Fihakhir, and A. Hafaifa, "Advanced sliding mode control for optimal grid integration of PV systems," *Energy Reports*, vol. 14, pp. 4246–4274, 2025, doi: 10.1016/j.egyr.2025.11.014.

[17] M. Gursoy, G. Zhuo, A. G. Lozowski, and X. Wang, "Photovoltaic energy conversion systems with sliding mode control," *Energies*, vol. 14, no. 19, pp. 1-20, 2021, doi: 10.3390/en14196071.

[18] Z. Sarra, M. Bouziane, R. Bouddou, H. Benbouhenni, S. Mekhilef, and Z.M.S. Elbarbary, "Intelligent control of hybrid energy storage system using NARX-RBF neural network techniques for microgrid energy management," *Energy Reports*, vol. 12, pp. 5445–5461, 2024, doi: 10.1016/j.egyr.2024.11.023.

[19] S. Zaidi, B. Meliani, R. Bouddou, S. M. Belhadj, and N. Bouchikhi, "Comparative study of different types of DC/DC converters for PV systems using RBF neural network-based MPPT algorithm," *Journal of Renewable Energies*, pp. 13–31, 2024, doi: 10.54966/jreen.v1i3.1291.

[20] S. M. Belhadj, B. Meliani, M. Rivera, P. Wheeler, E. Zerdali, and S. Zaidi, "Three-level DC-DC converter with fuzzy logic-based MPPT controller for photovoltaic applications," in *13th International Conference on Power Electronics, Machines and Drives (PEMD 2024)*, 2024, pp. 639–645, doi: 10.1049/icp.2024.2222.

[21] S. M. Belhadj, B. Meliani, H. Benbouhenni, S. Zaidi, Z.M.S. Elbarbary, and M. M. Alammar, "Control of multi-level quadratic DC-DC boost converter for photovoltaic systems using type-2 fuzzy logic technique-based MPPT approaches," *Heliyon*, vol. 11, no. 3, 2025, doi: 10.1016/j.heliyon.2025.e42181.

[22] B. Adda, M. Bouziane, A. Tayeb, H. Benbouenni, and Z. Sarra, "Enhancing Photovoltaic System Performance Through a Multi-Level Boost-Based Neural Network Optimization," *Studies in Science of Science*, vol. 43, no. 4, pp. 54–79, 2025.

[23] M. Venugopal, M. Mahadevaswamy, and M. B. S. Gowri, "Intelligent maximum power point tracking control for solar photovoltaic systems using fuzzy and neuro-fuzzy techniques," *Bulletin of Electrical Engineering and Informatics*, vol. 14, no. 6, pp. 4290–4303, 2025, doi: 10.11591/eei.v14i6.10735.

[24] M. V. Pham, "Adaptive Robust Control for Maximum Power Point Tracking in Photovoltaic Systems based on Sliding Mode and

Fuzzy Control," *International Journal of Electrical and Computer Engineering Systems*, vol. 16, no. 8, pp. 633–640, 2025, doi: 10.32985/ijeces.16.8.6.

[25] M. M. A. Rahman and M. M. A. Rahman, "A Single RBF Neural Network Approach to MPPT Algorithm for PV Systems," in *2024 IEEE International Conference on Electro Information Technology (eIT)*, Eau Claire, WI, USA, 2024, pp. 328–332, doi: 10.1109/eIT60633.2024.10609921.

BIOGRAPHIES OF AUTHORS

Anh Van Le was born in 1976 and received his Master's degree in Control Engineering and Automation from the University of Transport and Communications, Vietnam, in 2012. With a solid background in electrical systems and automation technologies, he has accumulated extensive experience in teaching and applied research. He is currently a lecturer in the Department of Industrial and Civil Electrical Engineering, Faculty of Electrical-Automation, University of Economics–Technology for Industries (UNETI), Hanoi, Vietnam. His main areas of research and professional interest include programmable logic controllers (PLC), the internet of things (IoT), the industrial internet of things (IIoT), and renewable energy systems. He has also participated in several projects related to automation applications and energy-efficient solutions. He can be contacted at email: lvanh@uneti.edu.vn.

Minh Van Pham obtained his Bachelor's degree in Electrical Engineering Technology, majoring in Automation, from the University of Economics–Technology for Industries (UNETI), Vietnam. In 2016, he earned his Master's degree in Control and Automation Engineering from the University of Transport, Vietnam. Since 2012, he has been a lecturer in the Department of Electrical Engineering, Faculty of Electrical-Automation, UNETI, Hanoi, Vietnam. With more than a decade of teaching and research experience, he has been actively involved in projects related to renewable energy systems and advanced control techniques. His primary research interests focus on intelligent control, robust adaptive control, wind energy conversion systems, and photovoltaic (solar) power generation. He is dedicated to developing efficient and reliable control solutions for sustainable energy applications. He can be contacted at email: pvminh@uneti.edu.vn.

Linh Thi To Vu graduated with an Engineer's degree in Automation Technology in 2011 from Nam Dinh University of Technology Education, Vietnam. In 2013, she earned her Master's degree in Control and Automation Engineering from the Military Technical Academy, Vietnam. From 2012 to 2024, she served as a lecturer in the Department of Electrical Engineering, Faculty of Electrical-Automation, University of Economics–Technology for Industries (UNETI), Hanoi, Vietnam. Throughout her academic career, she has been actively involved in teaching and research in the areas of automation systems and renewable energy applications. Her research interests include renewable energy technologies, intelligent control, and robust adaptive control systems. She is currently working in the Office of Administration and Management, where she continues to apply her expertise in technical coordination and organizational management. She can be contacted at email: vttlinh@uneti.edu.vn.